Environmental Science and Ecotechnology 21 (2024) 100428

Contents lists available at ScienceDirect

Environmental Science and Ecotechnology

journal homepage: www.journals.elsevier.com/environmental-science-and-ecotechnology/

Original Research

Polylactic acid micro/nanoplastic-induced hepatotoxicity: Investigating food and air sources via multi-omics

Hua Zha [a], Shengyi Han [a], Ruiqi Tang [a], Dan Cao [a], Kevin Chang [b], Lanjuan Li [a, *]

[a] State Key Laboratory for Diagnosis and Treatment of Infectious Diseases, National Clinical Research Center for Infectious Diseases, National Medical Center for Infectious Diseases, Collaborative Innovation Center for Diagnosis and Treatment of Infectious Diseases, The First Affiliated Hospital, Zhejiang University School of Medicine, Hangzhou, China

[b] Department of Statistics, The University of Auckland, Auckland, New Zealand

ARTICLE INFO

Article history:
Received 23 August 2023
Received in revised form
25 April 2024
Accepted 26 April 2024

Keywords:
Micro/nanoplastics
Hepatotoxicity
Microbiota dysbiosis
Metabolic disruption
Transcriptomic dysregulation

ABSTRACT

Micro/nanoplastics (MNPs) are detected in human liver, and pose significant risks to human health. Oral exposure to MNPs derived from non-biodegradable plastics can induce toxicity in mouse liver. Similarly, nasal exposure to non-biodegradable plastics can cause airway dysbiosis in mice. However, the hepatotoxicity induced by foodborne and airborne biodegradable MNPs remains poorly understood. Here we show the hepatotoxic effects of biodegradable polylactic acid (PLA) MNPs through multi-omics analysis of various biological samples from mice, including gut, fecal, nasal, lung, liver, and blood samples. Our results show that both foodborne and airborne PLA MNPs compromise liver function, disrupt serum antioxidant activity, and cause liver pathology. Specifically, foodborne MNPs lead to gut microbial dysbiosis, metabolic alterations in the gut and serum, and liver transcriptomic changes. Airborne MNPs affect nasal and lung microbiota, alter lung and serum metabolites, and disrupt liver transcriptomics. The gut Lachnospiraceae_NK4A136_group is a potential biomarker for foodborne PLA MNP exposure, while nasal unclassified_Muribaculaceae and lung *Klebsiella* are potential biomarkers for airborne PLA MNP exposure. The relevant results suggest that foodborne PLA MNPs could affect the "gut microbiota-gut-liver" axis and induce hepatoxicity, while airborne PLA MNPs could disrupt the "airway microbiota-lung-liver" axis and cause hepatoxicity. These findings have implications for diagnosing PLA MNPs-induced hepatotoxicity and managing biodegradable materials in the environment. Our current study could be a starting point for biodegradable MNPs-induced hepatotoxicity. More research is needed to verify and inhibit the pathways that are crucial to MNPs-induced hepatotoxicity.

1. Introduction

Micro/nanoplastics (MNPs) have been found in the environment and living organisms [1]. Polylactic acid (PLA), known for its high biocompatibility, is commonly utilized in food packaging materials [2], and PLA nanoplastics (NPs) can be released from commercial teabags [3]. PLA masks were found to release MNPs, which could enter the human airway [4]. A person was estimated to ingest 0.1–5 g MNPs weekly [5]. Therefore, airborne and foodborne PLA MNPs will likely influence human health.

NP and microplastics (MPs) could alter the gut microbiota in different living organisms. Fluorescent polystyrene (PS) MP exposure has been found to cause intestinal injury and gut microbiota dysbiosis (e.g., increased *Gordonia* and decreased *Aeromonas*) in zebrafish [6]. PS NP exposure could disrupt the gut microbiota in clams, e.g., enriched Vibrionaceae [7]. Oral exposure to polyethylene (PE) MPs could enrich *Staphylococcus* and inhibit *Parabacteroides* in the gut of mice [8]. The gut microbiota alternations induced by alternative common foodborne MNPs deserve further investigation.

Airborne PS MNPs have been found to induce airway dysbiosis. Nasal exposure to fluorescent PS MPs could cause pulmonary inflammatory cell infiltration and bronchoalveolar macrophage

* Corresponding author. State Key Laboratory for Diagnosis and Treatment of Infectious Diseases, National Clinical Research Center for Infectious Diseases, National Medical Center for Infectious Diseases, Collaborative Innovation Center for Diagnosis and Treatment of Infectious Diseases, The First Affiliated Hospital, Zhejiang University School of Medicine, 79 Qingchun Road, Hangzhou 310003, China.
E-mail address: ljli@zju.edu.cn (L. Li).

https://doi.org/10.1016/j.ese.2024.100428

aggregation in mice [9]. In the mice nasally exposed to PS MNPs, the abundances of lung unclassified_Muribaculaceae and nasal *Prevotella* were augmented by PS NPs, while lung *Roseburia* and nasal *Staphylococcus* were enriched by PS MPs [10]. PS NP exposure influenced the apoptosis, viability, and cell cycle of A549 human lung epithelial cells [11]. However, the airway toxicity of airborne biodegradable PLA MNPs remains poorly understood.

A few types of MNPs could induce or exacerbate hepatotoxicity. For instance, oral exposure to PS MPs was capable of causing inflammatory cell infiltration and hepatocyte edema in the liver of mice [12]. Polyethylene MP exposure could induce hepatocyte vacuolation and degeneration of nuclei in the liver of Nile tilapia [13]. Foodborne PS MP exposure could worsen cyclophosphamide-induced hepatotoxicity in mice [14]. Whether airborne MNPs could induce hepatotoxicity and foodborne biodegradable MNPs could cause hepatotoxicity is still unknown.

PLA MPs were found to be toxic to some living organisms. For instance, oral exposure to PLA MPs caused gut damage and microbial dysbiosis in zebrafish [15]. Oral exposure to PLA MPs could induce neurotoxic effects and REDOX imbalance in dragonfly larvae [16]. The alternative toxicity of PLA MNPs needs to be further explored before more widespread application of PLA.

It is hypothesized that foodborne PLA MNP exposure could induce alterations in gut microbiota, gut and serum metabolome and lead to liver transcriptomic changes and hepatoxicity, while airborne PLA MNP exposure could induce alterations in airway microbiota, lung and serum metabolome and lead to liver transcriptomic changes and liver toxicity. Therefore, in the current study, we aim to determine (1) whether foodborne biodegradable PLA MNPs could affect the “gut microbiota-gut-liver” axis and induce hepatotoxicity and (2) whether airborne biodegradable PLA MNPs could disrupt the “airway microbiota-lung-liver” axis and cause hepatotoxicity.

2. Materials and methods

2.1. Animal experiments

Sixty male Institute of Cancer Research (ICR) mice (four-week-old, pathogen-free), PLA NP (50 nm), and MP (5 μm) were purchased and prepared for this study. Mice were allocated randomly to six groups, i.e., foodborne NP (FQ), foodborne MP (FR), foodborne control (FNC), airborne NP (AQ), airborne MP (AR), and airborne control (ANC) groups ($n = 10$ per group). They were kept at 22 °C under light/dark (12:12) cycles for seven days to adapt to the environment.

In the foodborne MNP section, a 100-μL aliquot of sterile water with 0.2 mg NPs, 0.2 mg MP, and 0 mg MNPs was administered orally to each mouse in the FQ, FR, and FNC groups. Oral gavage was conducted every day for six weeks before anesthetizing the mice to collect blood, liver, feces, and colon.

In the airborne MNP section, a 10-μL aliquot of sterile saline with 0.03 mg NPs, 0.03 mg MP, and 0 mg MNPs was intranasally administered for each mouse in the AQ, AR, and ANC groups, respectively [9]. The nasal exposure was performed once every third day for 42 days before anesthetizing the mice to collect nasal tissue, lung, liver, and blood. The work was permitted by the Animal Care and Use Committee of Zhejiang University (2021-945).

2.2. Measurement of biochemical variables

Serum extraction was performed via centrifugation. The liver function variables, i.e., aspartate aminotransferase (AST) and alanine aminotransferase (ALT), and the antioxidant biomarkers, i.e., total antioxidant capacity (T-AOC) and superoxide dismutase (SOD), in the serum of all the mice, were measured with commercial assay kits according to the manufacturer's protocols.

2.3. Histology analysis

Formalin (10%) was used to fix the colon and liver of FQ, FR, and FNC groups and the lung and liver of AQ, AR, and ANC groups. Standard histological methods were used to process the fixed tissues. The stained samples were mounted on the microscope slides to assess pathological changes.

2.4. Molecular experiments and data processing

The fecal, nasal, and lung samples were processed for DNA extraction using a DNA isolation kit. The 16S rDNA V3−V4 region of the extracted DNA was amplified by the bacterial primers (341F/785R) [17]. Polymerase chain reaction (PCR) products were purified before being sent to the sequencing lab for Illumina sequencing. Standard procedures were used to process the sequencing data, and sequences were clustered into different amplicon sequence variants (ASVs) [18]. Taxonomy assignment was performed for the filtered ASVs against the Silva 138 database [19]. The details are provided in Supplementary Materials.

2.5. Microbiota composition analyses

The main phyla and families in the gut microbiota of FQ, FR, and FNC groups, and in the nasal and lung microbiota of AQ, AR, and ANC groups, were determined. The alpha diversity indices of the gut, nasal, and lung microbiota were calculated. Permutational analysis of variance (PERMANOVA) was performed to compare the gut microbiota compositions of foodborne groups and to compare airborne groups for their lung and nasal microbiota compositions.

Principal coordinate analysis (PCoA) and non-metric multidimensional scaling (nMDS) were carried out to demonstrate the gut microbiota of FQ, FR, and FNC groups and the nasal and lung microbiota of AQ, AR, and ANC groups. Similarity percentage (SIMPER) analysis was performed to investigate the gut microbiota similarities in foodborne groups and airway microbiota similarities in airborne groups. Linear discriminant analysis effect size (LEfSe) was used to compare foodborne groups for the gut microbiota and airborne groups for their airway microbiota.

2.6. Microbiota network analyses

Co-occurrence network inference (CoNet) analysis was carried out to determine the microbiota networks in the gut of FQ, FR, and FNC groups, as well as those in the nasal tissue and lung of AQ, AR, and ANC groups. Network fragmentation analysis was conducted to explore the structural gatekeepers in the gut microbiota networks of FQ, FR, and FNC groups, and those in the nasal and lung microbiota networks of AQ, AR, and ANC groups. The details are provided in Supplementary Materials.

2.7. Microbial function analyses

The gut microbial functional profiles of FQ, FR, and FNC groups, as well as the nasal and lung microbial functional profiles of AQ, AR, and ANC groups, were predicted using the PICRUSt2 pipeline. Statistical Analysis of Metagenomic Profiles (STAMP) was carried out to investigate (1) the gut microbial pathways upregulated in the FQ and FR groups, (2) the airway microbial pathways upregulated in the AQ and AR groups, and (3) the microbial pathways differed between MP and NP groups.

2.8. Metabolite extraction, profiling, and analyses

Serum, colon, and lung were processed for untargeted metabolomic analysis (ten mice in each group). Principal component analysis (PCA) was carried out to demonstrate the metabolic profiles. Orthogonal partial least squares-discriminant analysis (OPLS-DA) was performed to explore the metabolites that differed between groups. Pathway enrichment analysis determined the enriched pathways in the foodborne and airborne MNP groups. The details are provided in Supplementary Materials.

2.9. Transcriptome analyses

RNA was extracted from liver samples (ten mice in each group) and submitted for transcriptome sequencing on the Illumina platform. Principal component analysis (PCA) was used to visualize the gene expression profiles of different groups. Differential expression analysis was conducted to determine the differentially expressed genes (DEGs). Afterwards, DEGs were submitted for Gene Ontology (GO) and Kyoto Encyclopedia of Genes and Genomes (KEGG) enrichment analyses. The details are provided in Supplementary Materials.

2.10. Pathway analyses

Venny analysis was carried out to determine the pathways commonly enriched in the gut, serum, and/or liver of the FQ group and those of the FR group. The same strategy was performed to investigate the pathways commonly enhanced in the lung, serum, and/or liver of the AQ group and those of the AR group. The liver pathways commonly enriched in the FQ, FR, AQ, and AR groups were also explored.

2.11. Integrated analyses of altered microbiota, metabolome, and transcriptome data

The correlations between the altered components (i.e., microbes, metabolites, and transcripts) in the corresponding MNP groups were investigated using CoNet analysis and were demonstrated using Cytoscape. The sub-networks with only one type of component were filtered before the fragmentation analysis was conducted to determine the correlation gatekeepers in the correlation networks of the MNP groups. The key correlation gatekeeper in each group is defined as the component(s) associating with most alternative types of components. The details are provided in Supplementary Materials.

2.12. Statistical analysis

Statistical analysis was performed in IBM SPSS statistics 25, and statistical significance was set at $P < 0.05$. Non-parametric and parametric methods were carried out as appropriate.

3. Results

3.1. MNPs affected liver function and antioxidant activity

Both serum AST and ALT were at higher levels in the FQ and FR groups than in the FNC group (Fig. 1a and b). Serum SOD was similar between the three groups (Fig. 1c), while serum T-AOC was decreased in the FQ and FR groups (Fig. 1d). In the nasal exposure section, serum AST and ALT were elevated in both AQ and AR groups (Fig. 1e and f). SOD was reduced in the AQ group but was not significantly altered in the AR group (Fig. 1g). By contrast, no significant difference was determined in serum T-AOC between AQ, AR, and ANC groups (Fig. 1h).

3.2. MNPs caused liver and lung pathology

Hepatocyte swelling, spotty necrosis, cell vacuolization, and karyopyknosis were determined in the liver of FQ and FR groups (Fig. 1i). In contrast, no obvious pathological change was observed in the colon of the foodborne MNP and control groups (Supplementary Materials Fig. S1). In the nasal exposure section, hemorrhage, inflammatory cell infiltration, and exudates were observed in the lung of AQ and AR groups (Fig. 1j). Hepatocyte swelling, cell vacuolization, and karyopyknosis were determined in the liver of AQ and AR groups (Fig. 1k).

3.3. Foodborne MNPs altered gut microbiota

3.3.1. Foodborne MNPs changed gut microbiota composition

Firmicutes was the most abundant bacterial phylum accounting for over 60% of gut microbiota in the FQ, FR, and FNC groups (Fig. 2a). The bacterial family Lachnospiraceae had the greatest abundance in both FQ and FR groups, while Lactobacillaceae was the most abundant bacterial family in FNC group (Fig. 2b). Alpha diversity of gut microbiota was similar between FQ, FR, and FNC groups (Fig. 2c–e). Average similarity within gut microbiota was lower in the FQ (42.88%) and FR (34.7%) groups compared to the FNC group (52.31%).

A significant difference was determined between the gut microbiota compositions of FQ, FR, and FNC groups based on PERMANOVA results ($R^2 = 0.18$, $P < 0.001$) and was visualized by PCoA and nMDS plots (Fig. 2f and g). The gut microbiota composition was greatly altered in both FQ and FR groups ($R^2 > 0.17$, $P < 0.003$). LEfSe determined multiple gut bacteria associated with FQ and FR groups, among which Lachnospiraceae_NK4A136_group, Lachnospiraceae_A2, and *Helicobacter* were most associated with FQ group (Fig. 2h), while Lachnospiraceae_NK4A136_group, *Roseburia*, and *Helicobacter* were most associated with FR group (Fig. 2i). Eight gut bacteria were commonly enriched in both FQ and FR groups, among which Lachnospiraceae_NK4A136_group was most enriched (Supplementary Materials Table S1).

3.3.2. Foodborne MNPs altered gut microbiota networks

The five gut bacterial phylotypes with the most correlations in the networks of the three foodborne groups were determined (Supplementary Materials Table S2, Fig. S2), among which a Lachnospiraceae_NK4A136_group phylotype had the most correlations in both FQ and FR gut networks. Nine phylotypes assigned to Lachnospiraceae_NK4A136_group, Muribaculaceae, Lachnospiraceae, and Oscillospiraceae were determined as gatekeepers in the FQ gut network (Fig. 2j). Eleven phylotypes assigned to *Colidextribacter*, *Roseburia*, Lachnospiraceae_ASF356, Lachnospiraceae_NK4A136_group, Lachnospiraceae, Oscillospiraceae, and Clostridia_vadinBB60_group were found as structural gatekeepers in the FR gut network (Fig. 2k).

3.3.3. Foodborne MNPs altered gut microbial functional pathways

A variety of gut microbial functional pathways were upregulated in the FQ and FR groups, among which “ABC transporters”, “flagellar assembly”, and “bacterial chemotaxis” were most upregulated in both of the two groups (Supplementary Materials Fig. S3).

3.4. Airborne MNPs changed nasal microbiota

3.4.1. Airborne MNPs altered nasal microbiota composition

At the phylum level, Firmicutes was most abundant in the AQ,

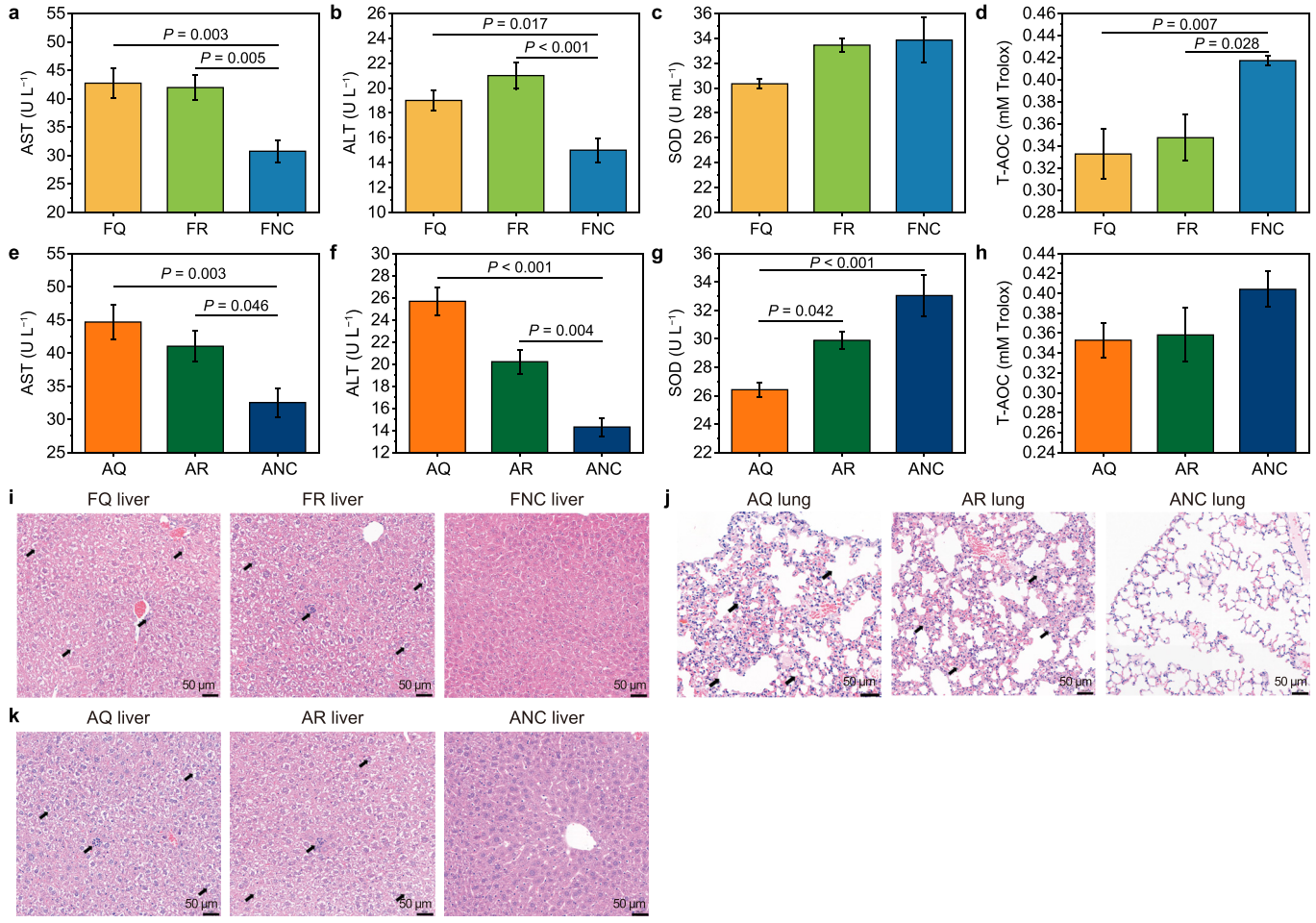

Fig. 1. Serum biochemical parameters and histological changes in the PLA MNPs-exposed groups. **a**–**d**, Serum AST (**a**), ALT (**b**), SOD (**c**), and T-AOC (**d**) in foodborne NP (FQ), foodborne MP (FR), and foodborne control (FNC) groups. **e**–**h,** Serum AST (**e**), ALT (**f**), SOD (**g**), and T-AOC (**h**) in airborne NP (AQ), airborne MP (AR), and airborne control (ANC) groups. i, Liver histology in the FQ, FR, and FNC groups. **j**–**k,** Lung (**j**) and liver (**k**) histology in the AQ, AR, and ANC groups. Black arrows point at the histological changes in tissues.

AR, and ANC groups, constituting over 50% of nasal microbiota in each of the three groups (Fig. 3a). Staphylococcaceae was the most abundant nasal family in the AQ, AR, and ANC groups (Fig. 3b). Nasal alpha diversity indices were all at higher levels in both the AQ and AR groups than in ANC group (Fig. 3c–e). The average similarity within nasal microbiota was slightly higher in the AQ (18.36%) and AR (22.22%) groups compared to the ANC group (17.36%).

PERMANOVA determined the nasal microbiota composition was different between AQ, AR, and ANC groups ($R^2 = 0.12$, $P < 0.001$), and both AQ and AR groups were different from the ANC group (Both $R^2 > 0.09$, both $P < 0.006$). The nasal microbiota difference was visualized in PCoA and nMDS plots (Fig. 3f and g). Multiple nasal bacteria were associated with AQ and AR groups (Fig. 3h and i), of which unclassified_Muribaculaceae, Lachnospiraceae_NK4A136_group, and *Acinetobacter* were greatly upregulated in the AQ group (Fig. 3h), while unclassified_Muribaculaceae, *Lactobacillus*, and *Sporosarcina* were largely upregulated in the AR group (Fig. 3i). There were 20 nasal bacteria upregulated in both AQ and AR groups, among which unclassified_Muribaculaceae was the most enriched one (Supplementary Materials Table S3).

3.4.2. Airborne MNPs altered nasal microbiota networks

The nasal phylotypes with the most correlations in the airborne groups were determined (Supplementary Materials Table S4, Fig. S4), among which two phylotypes assigned to *Prevotella* and *Pelomonas* had the most correlations in the AQ and AR nasal networks, respectively. Two *Alistipes* and *Lachnoclostridium* phylotypes were determined as the structural gatekeepers in the AQ nasal network (Fig. 3j), while two structural gatekeepers assigned to *Escherichia-Shigella* and *Sphingomonas* were found in the AR nasal network (Fig. 3k).

3.4.3. Airborne MNPs altered nasal microbial functional pathways

Multiple functional pathways of nasal microbiota were upregulated in the AQ and AR groups, among which "flagellar assembly", "bacterial chemotaxis", and "cell cycle − caulobacter" were most upregulated in both the two groups (Supplementary Materials Fig. S5).

3.5. Airborne MNPs altered lung microbiota

3.5.1. Airborne MNPs changed lung microbiota composition

At the phylum level, Firmicutes and Proteobacteria were most abundant in the lung microbiota of AQ and AR groups, while Firmicutes and Bacteroidota had the greatest abundances in the lung microbiota of ANC group (Fig. 4a). Enterobacteriaceae, Muribaculaceae, and Lachnospiraceae constituted more than 30% of lung microbiota In the AQ and AR groups, while Muribaculaceae, Lachnospiraceae, and Staphylococcaceae were the three most abundant lung bacterial families in ANC group (Fig. 4b). Lung

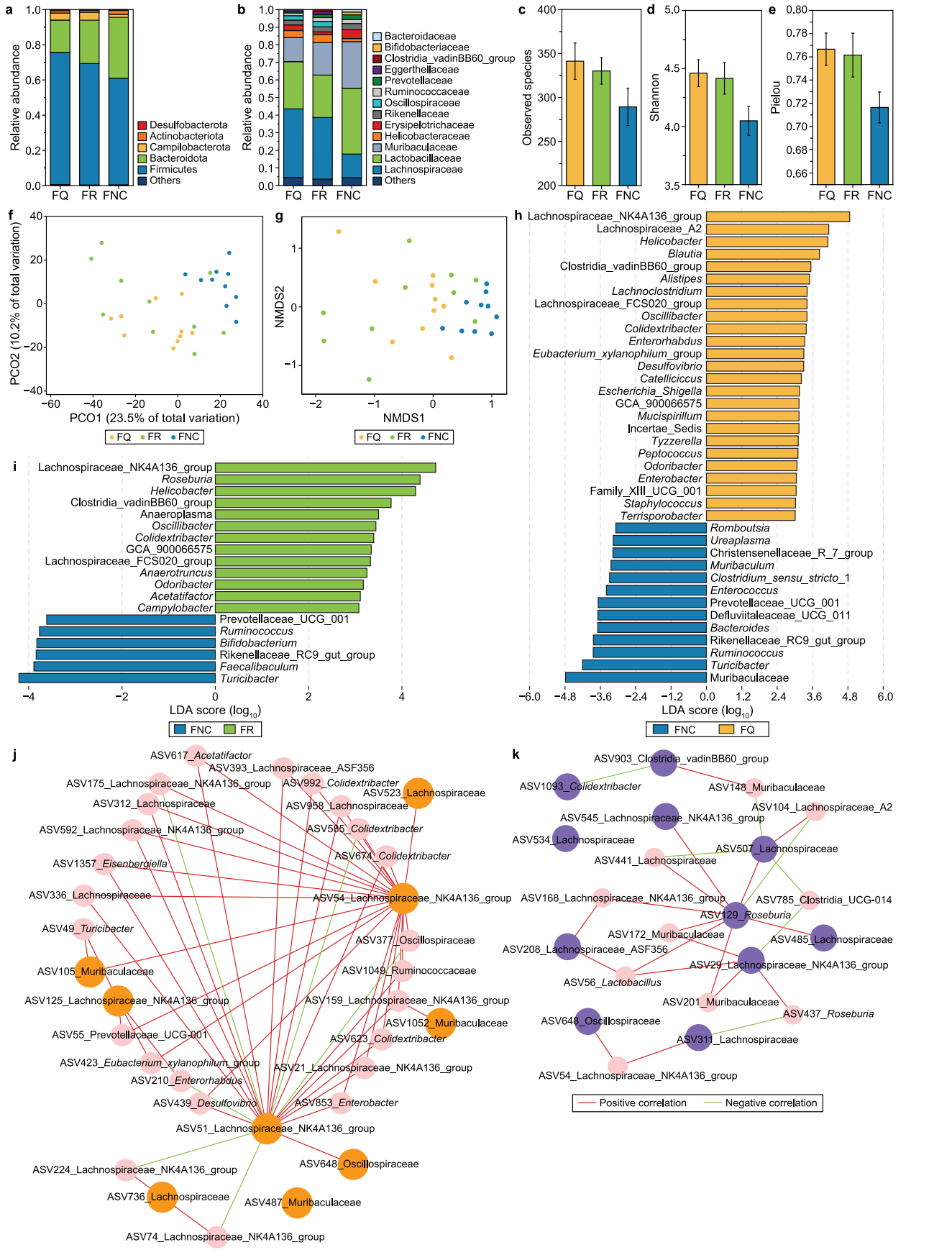

Fig. 2. Main components and alpha diversity indices of gut microbiota in foodborne PLA MNP and control groups. **a**–**b**, Major gut bacterial phyla (**a**) and families (**b**). **c**–**e**, Gut microbial richness (**c**), diversity (**d**), and evenness (**e**) indices. **f**–**g**, PCoA (**f**) and nMDS (**g**) plots of gut microbiota. h, Differential gut bacteria between FQ and FNC groups. i, Differential gut bacteria between FR and FNC groups. **j**–**k**, Structural gatekeepers in the FQ (**j**) and FR (**k**) gut microbiota networks.

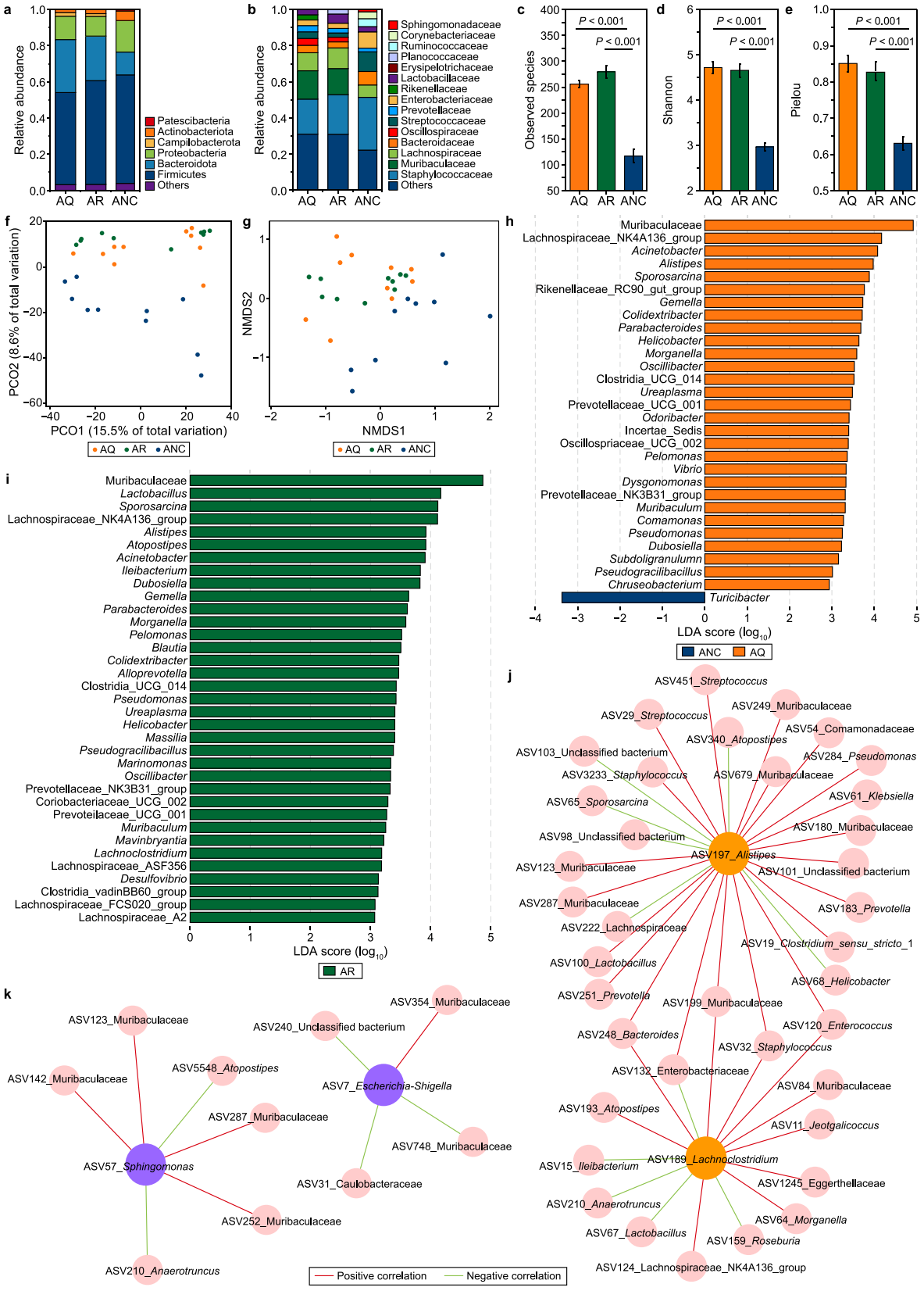

Fig. 3. Main components and alpha diversity indices of nasal microbiota in airborne PLA MNP and control groups. **a**–**b**, Major nasal bacterial phyla (**a**) and families (**b**). **c**–**e**, Nasal microbial richness (**c**), diversity (**d**), and evenness (**e**) indices. **f**–**g**, PCoA (**f**) and nMDS (**g**) plots of nasal microbiota. h, Differential nasal bacteria between AQ and ANC groups. **i**, Differential nasal bacteria between AR and ANC groups. **j**–**k**, Structural gatekeepers in the AQ (**j**) and AR (**k**) nasal microbiota networks.

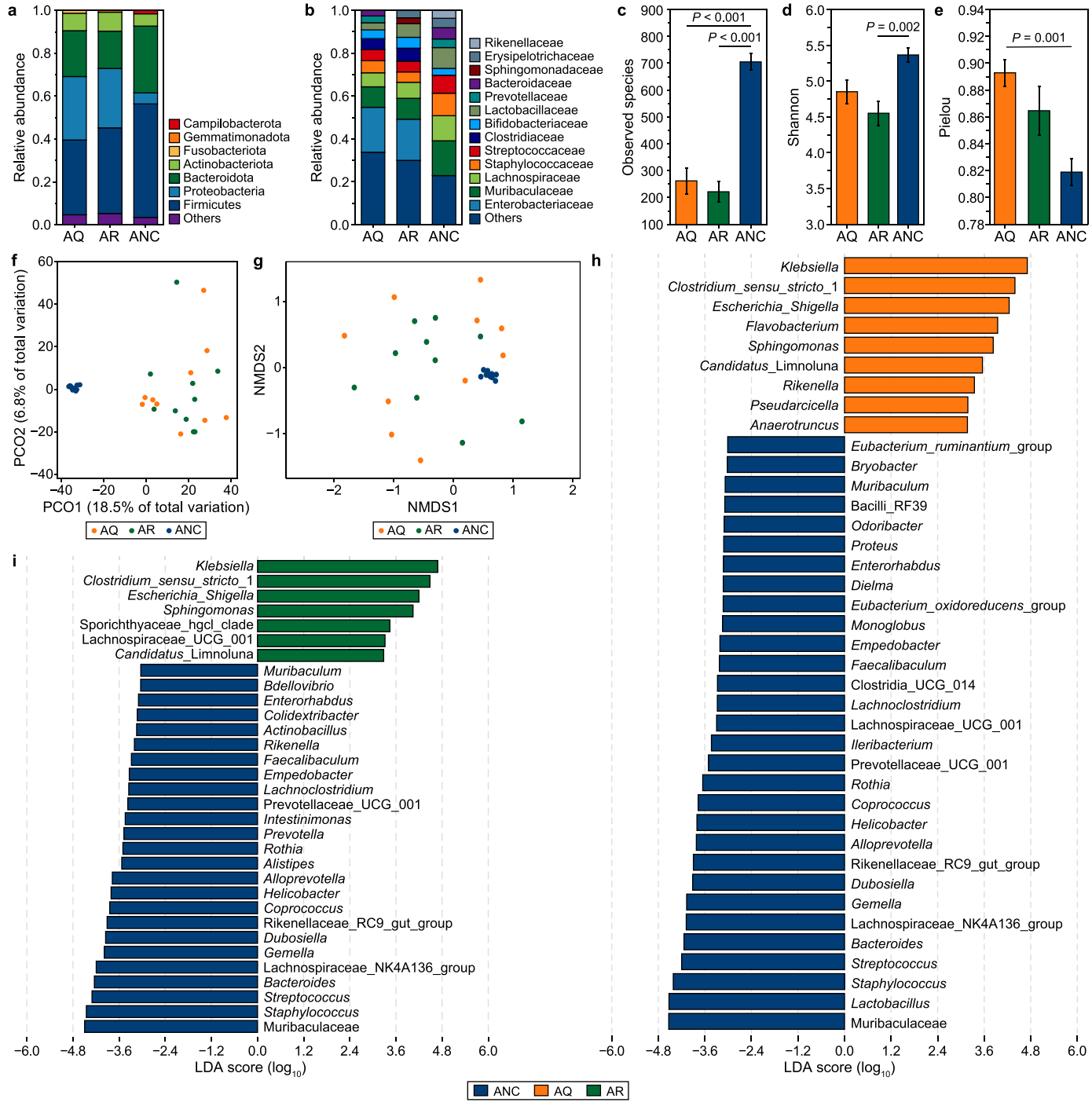

Fig. 4. Main components and alpha diversity indices of lung microbiota in airborne PLA MNP and control groups. **a**–**b**, Major lung bacterial phyla (**a**) and families (**b**). **c**–**e**, Lung microbial richness (**c**), diversity (**d**), and evenness (**e**) indices. **f**–**g**, PCoA (**f**) and nMDS (**g**) plots of lung microbiota. h, Differential lung bacteria between AQ and ANC groups. **i**, Differential lung bacteria between AR and ANC groups. **j**, Differential lung microbial pathways between AQ and ANC groups. **k**, Differential lung microbial pathways between AR and ANC groups.

bacterial observed species were lower in both AQ and AR groups compared to ANC group (Fig. 4c). Reduced Shannon index was determined in the AR group (Fig. 4d), while elevated Pielou index was found in the AQ group (Fig. 4e). The average similarity of lung microbiota was decreased in the AQ and AR groups compared to ANC group, i.e., 8.02%, 9.81%, and 49.34%, respectively.

PERMANOVA results indicated the lung microbiota composition was different between AQ, AR, and ANC groups ($R^2 = 0.2$, $P < 0.001$), which was visualized in PCoA and nMDS plots (Fig. 4f and g). Compared with the ANC group, both AQ and AR groups had altered lung microbiota compositions ($R^2 > 0.22$, $P < 0.001$). Multiple lung bacteria were associated with AQ and AR groups (Fig. 4h and i), and five were commonly enriched in both AQ and AR groups (Supplementary Materials Table S5). *Klebsiella*, *Clostridium_sensu_stricto*_1, and *Escherichia-Shigella* were most associated with both groups.

3.5.2. MNPs altered lung microbiota networks

The five lung bacterial phylotypes with the most correlations in the three groups were determined (Supplementary Materials Table S6, Fig. S6), of which two phylotypes assigned to *Klebsiella* and Muribaculaceae had the most correlations in the AQ and AR lung networks, respectively. No structural gatekeeper was found in the AQ or AR lung networks.

3.5.3. Airborne MNPs altered lung microbial functional pathways

Various lung microbial functional pathways were upregulated in the AQ and AR groups (Supplementary Materials Fig. S7a and b). "Flagellar assembly", "porphyrin and chlorophyll metabolism", and "phenylalanine metabolism" were most upregulated in the AQ group (Supplementary Materials Fig. S7a), while "flagellar assembly", "bacterial chemotaxis", and "phenylalanine metabolism" were most upregulated in the AR group (Supplementary Materials Fig. S7b).

3.6. Foodborne MNPs-induced gut and serum metabolic alterations

Variations were found in the gut metabolic profile between FQ, FR, and FNC groups (Supplementary Materials Fig. S8a). There were 752 and 637 altered gut metabolites in the FQ and FR groups, respectively (Fig. 5a and b). Similarly, variations were determined between the serum metabolic profiles of FQ, FR, and FNC groups (Supplementary Materials Fig. S8b). A total of 832 and 753 serum metabolites were altered in the FQ and FR groups, respectively (Fig. 5c and d).

The altered gut metabolites were mainly related to intensified pathways such as "steroid hormone biosynthesis", "central carbon metabolism in cancer", and "ABC transporters" in the FQ group; and "central carbon metabolism in cancer", "protein digestion and absorption", and "aminoacyl-tRNA biosynthesis" in the FR group (Fig. 5e). A total of 18 gut pathways were enriched in both FQ and FR groups, among which "central carbon metabolism in cancer" was most upregulated (Fig. 5e).

Serum pathways such as "linoleic acid metabolism", "arachidonic acid metabolism", and "tryptophan metabolism" were enriched in the FQ group, while serum pathways such as "linoleic acid metabolism", "drug metabolism − other enzymes", and "tryptophan metabolism" (Fig. 5f). Four serum pathways were enhanced in both FQ and FR groups, among which "linoleic acid metabolism" was the most enriched one (Fig. 5f).

3.7. Foodborne MNPs-induced liver transcriptomic alterations

Some variations were determined in the liver transcriptomic profile between FQ, FR, and FNC groups (Supplementary Materials Fig. S8c). There were 307 and 262 liver DEGs altered in the FQ and FR groups, respectively (Fig. 5g and h). Three liver GO terms respectively belonging to biological process, cellular component, and molecular function, i.e., negative regulation of chromatin silencing, extracellular region, and nucleosomal DNA binding, were largely enriched in the FQ group (Fig. 5i), while nucleosome assembly was most enriched (Fig. 5j). Two different groups of nine liver pathways were enriched in the FQ and FR groups, among which "circadian rhythm" was most upregulated in both FQ and FR groups (Fig. 5k).

3.8. Airborne MNPs-induced lung and serum metabolic alterations

PCA showed variations in the lung metabolic profile between AQ, AR, and ANC groups (Supplementary Materials Fig. S9a). There were 864 and 596 lung metabolites respectively elevated in the AQ and AR groups (Fig. 6a and b). The serum metabolic profile differed in the AQ, AR, and ANC groups (Supplementary Materials Fig. S9b). There were 503 and 664 serum metabolites altered in the AQ and AR groups, respectively (Fig. 6c and d).

The altered lung metabolites were mainly related to pathways such as "steroid hormone biosynthesis", "arachidonic acid metabolism", and "purine metabolism" in the AQ group; and "arachidonic acid metabolism", "steroid hormone biosynthesis", and "choline metabolism in cancer" in the AR group (Fig. 6e). Nine lung pathways were enriched in both AQ and AR groups, of which "arachidonic acid metabolism" was most upregulated (Fig. 6e).

Serum pathways such as "central carbon metabolism in cancer", "alanine, aspartate and glutamate metabolism", "butanoate metabolism", and "protein digestion and absorption" were upregulated in the AQ group, while serum pathways such as "protein digestion and absorption", "tryptophan metabolism", "phenylalanine, tyrosine and tryptophan biosynthesis", and "central carbon metabolism in cancer" were enriched in the AR group (Fig. 6f). There were 11 serum pathways enriched in both AQ and AR groups, of which "central carbon metabolism in cancer" and "protein digestion and absorption" were largely enhanced (Fig. 6f).

3.9. Airborne MNPs-induced liver transcriptomic alterations

Great variations were found in the liver transcriptomic profile between AQ, AR, and ANC groups (Supplementary Materials Fig. S9c). Two groups of 303 and 289 liver DEGs were changed in the AQ and AR groups, respectively (Fig. 6g and h). "Nucleosome assembly" was the most upregulated liver GO term in both AQ and AR groups (Fig. 6i and j). Multiple liver pathways were upregulated in the AQ and AR groups, among which "alcoholism", "systemic lupus erythematosus", and "neutrophil extracellular trap formation" were largely upregulated in both groups (Fig. 6k).

3.10. Pathway analysis

"Arginine biosynthesis" and "arachidonic acid metabolism" were enriched in both the gut and serum of the FQ group (Supplementary Materials Fig. S10a), while "antifolate resistance" was enhanced in both gut and serum of the FR group (Supplementary Materials Fig. S10b). In the AQ group, "biosynthesis of unsaturated fatty acids" was enriched in both lung and liver, while "mineral absorption" was upregulated in both serum and liver (Supplementary Materials Fig. S10c). Similarly, in the AR group, the "mTOR signaling pathway" was intensified in both lung and serum, while the "FoxO signaling pathway" was enhanced in both lung and liver (Supplementary Materials Fig. S10d).

"Circadian rhythm" was commonly enriched in the liver of FQ, FR, AQ, and AR groups (Supplementary Materials Fig. S10e). Three enriched DEGs, i.e., *Arntl*, *Cry1*, and *Npas2*, were commonly upregulated in "circadian rhythm" in the four groups (Supplementary Materials Table S7).

3.11. Correlation networks in MNP groups

The four correlation networks composed of altered microbes, metabolites, and transcripts in the MNP groups were determined (Fig. 7a–d) and the multiple corresponding correlation gatekeepers (Supplementary Materials Tables S8–S11). The DEG *Gm1673* was the key correlation gatekeeper correlating with 23 components belonging to alternative types in the FQ group (Fig. 7e). The DEGs *cyp2b9* and *klhdc7b*, and serum metabolite bacterioruberin diglucoside were the key correlation gatekeepers in the FR group (Fig. 7f). The DEG *zfp804b* and gut metabolite 11-cis-3,4-didehydroretinol were the key correlation gatekeepers in the AQ and AR groups, respectively (Fig. 7g and h).

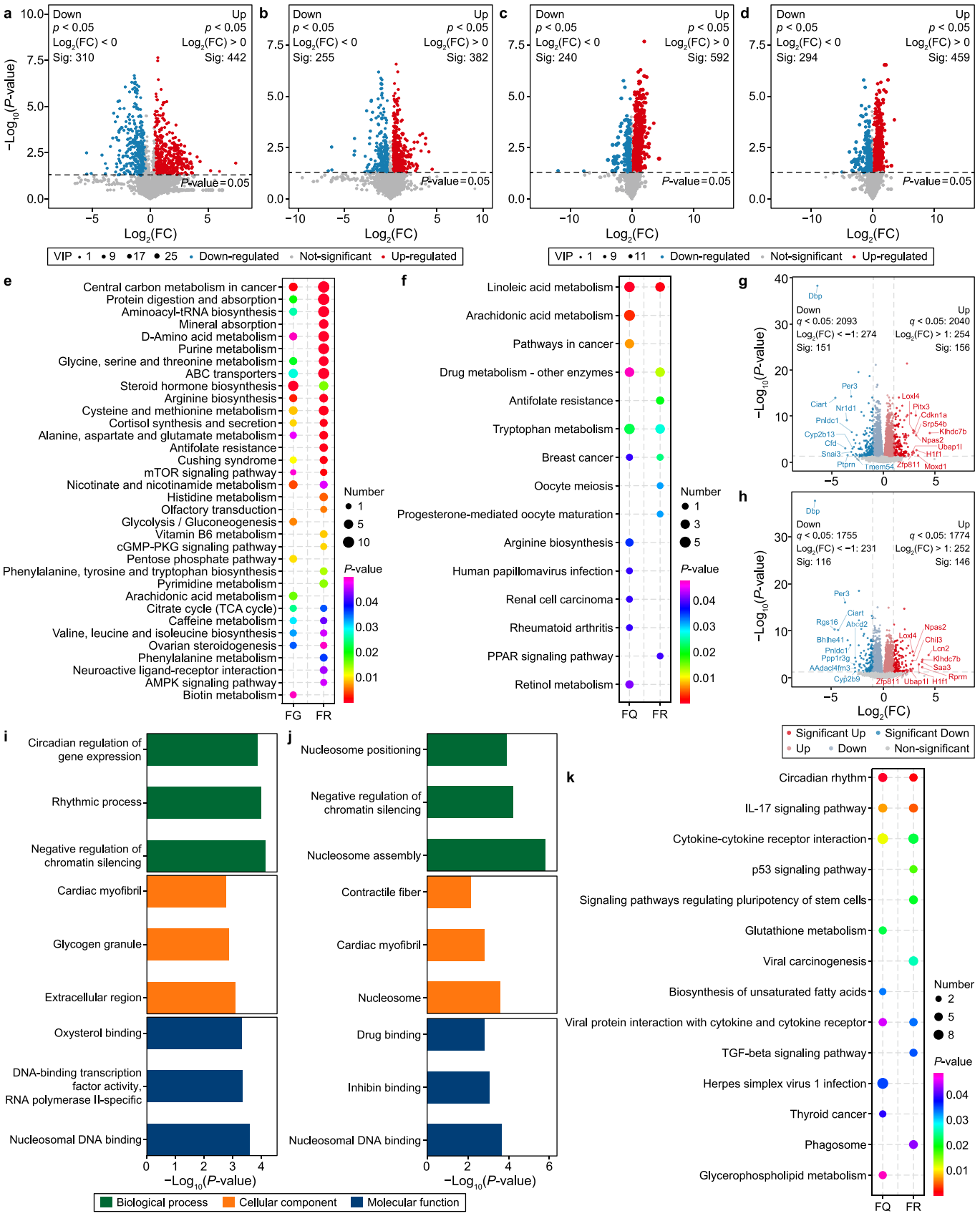

Fig. 5. Metabolic and transcriptomic alterations induced by foodborne PLA NPs and MPs. **a**–**b**, Alterations of gut metabolites in the FQ (**a**) and FR (**b**) groups. **c**–**d**, Alterations of serum metabolites in the FQ (**c**) and FR (**d**) groups. **e**–**f**, Enriched gut pathways (**e**) and serum pathways (**f**) in the FQ and FR groups. **g**–**h**, Altered liver transcripts in the FQ (**g**) and FR (**h**) groups. **i**–**j**, Enriched liver GO terms FQ (***i***) and FR (**j**) groups. **k**, Enriched liver pathways in the FQ and FR groups.

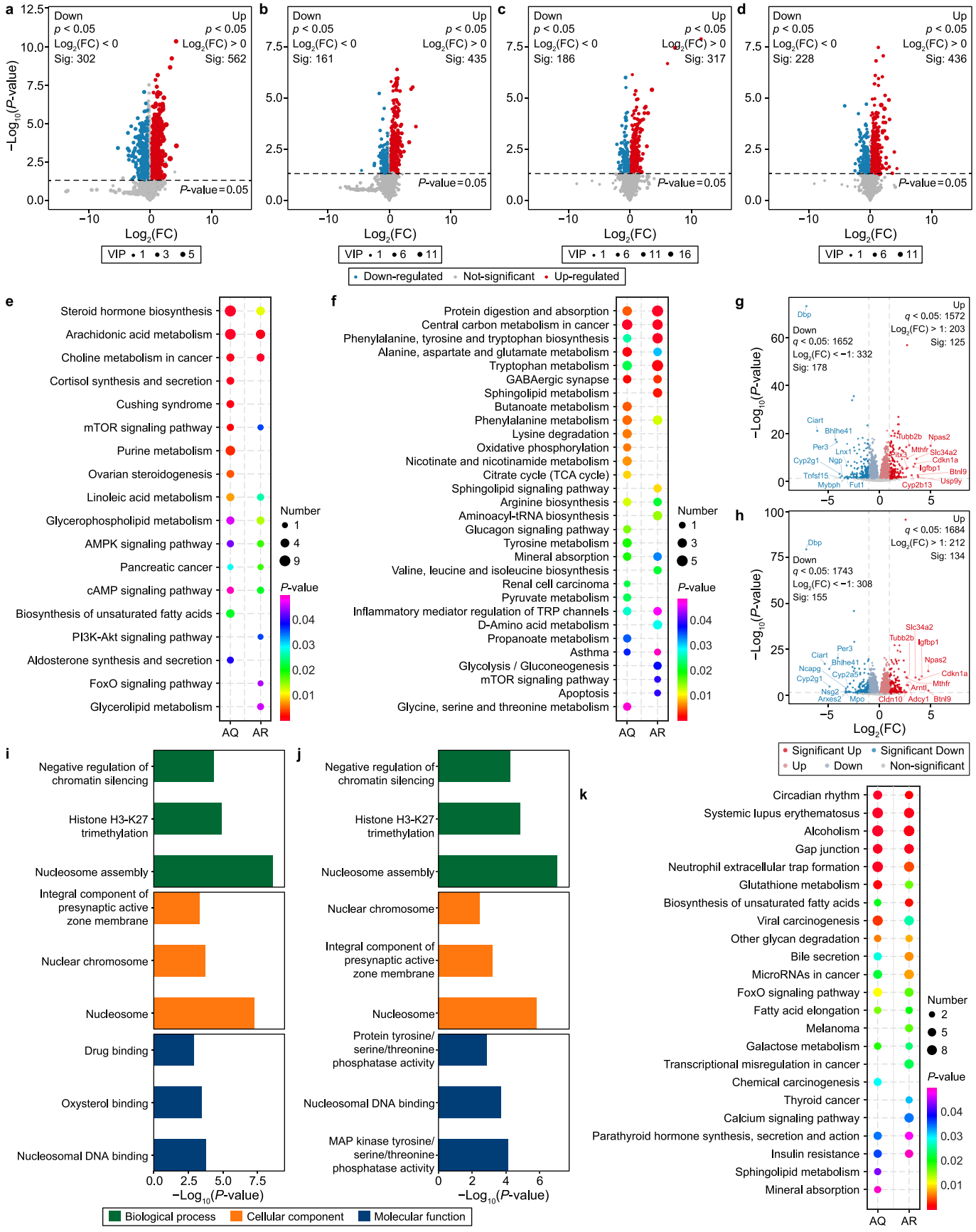

Fig. 6. Metabolic and transcriptomic alterations induced by airborne PLA NPs and MPs. **a**–**b**, show the altered lung metabolites in the AQ (**a**) and AR (**b**) groups. **c**–**d**, Alterations of serum metabolites in the AQ (**c**) and AR (**d**) groups. **e**–**f**, Enriched lung pathways (**e**) and serum pathways (**f**) in the AQ and AR groups. **g**–**h**, show altered liver transcripts in the AQ (**g**) and AR (**h**) groups. **i**–**j**, show enriched liver GO terms in the AQ (**i**) and AR (**j**) groups. **k**, Enriched liver pathways in the AQ and AR groups.

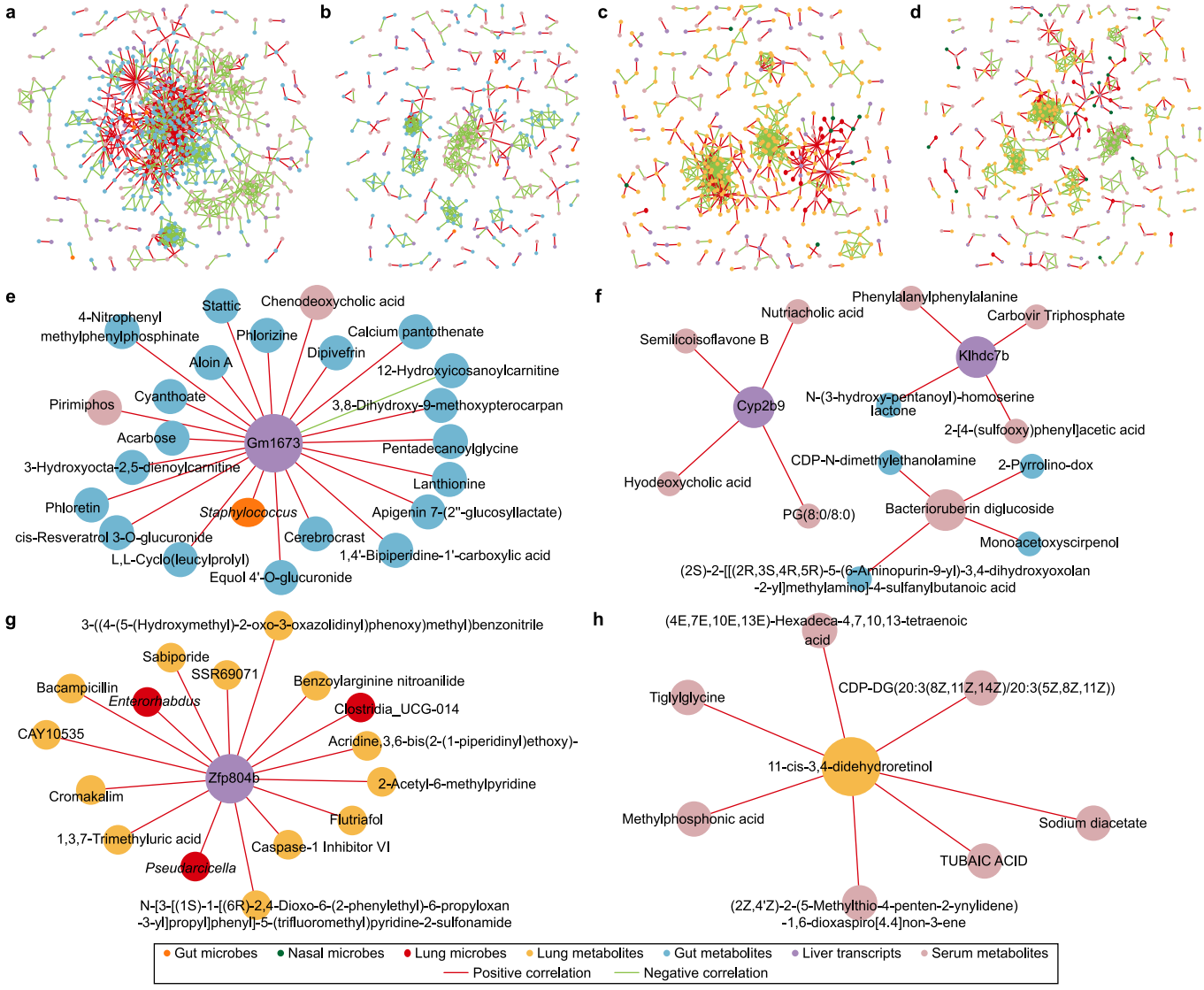

Fig. 7. Correlation networks and the correlation gatekeepers in PLA MNPs-exposed groups. **a**–**d**, Correlation networks of altered microbes, metabolites, and liver transcripts in the FQ (**a**), FR (**b**), AQ (**c**), and AR (**d**) groups. **e**–**h**, Key correlation gatekeepers (larger-sized) and the correlated alternative types of components (smaller-sized) in the FQ (**e**), FR (**f**), AQ (**g**), and AR (**h**) groups.

3.12. Multi-omics analysis determined the dissimilarities between NP and MP exposures

3.12.1. Dissimilarities between foodborne NP and MP groups

There were 11 gut bacteria and 17 gut microbial pathways differentiating FQ and FR groups, among which Lachnospiraceae_A2 and "ABC transporters" could largely distinguish the FQ group from the FR group, while *Roseburia* and "oxidative phosphorylation" could greatly differentiate FR group from FQ group (Supplementary Materials Fig. S11a and b). A total of 273 gut metabolites differed between the FQ and FR groups, among which 174 were more elevated in the FQ group, while 99 were at higher levels in the FR group (Supplementary Materials Fig. S11c). Six gut pathways were at different levels between the FQ and FR groups, all of which were more intensified in the FQ group (e.g., "glycolysis/gluconeogenesis") (Supplementary Materials Fig. S11d). A total of 267 serum metabolites differed between FQ and FR groups, among which 175 were more elevated in the FQ group, and 92 were more elevated in the FR group (Supplementary Materials Fig. S11e). These differential serum metabolites were mainly involved in serum pathways such as "glycerophospholipid metabolism" and "arachidonic acid metabolism" more upregulated in the FQ group (Supplementary Materials Fig. S11f), and serum pathways such as "choline metabolism in cancer" more upregulated in the FR group (Supplementary Materials Fig. S11g)). Multiple liver DEGs and differential GO terms were determined between FQ and FR groups (Supplementary Materials Fig. S11h and i), and they were mainly related to 12 differential liver pathways, among which "acute myeloid leukemia" and "retinol metabolism" were greatly intensified in the FQ and FR groups, respectively (Supplementary Materials Fig. S11j and k).

3.12.2. Dissimilarities between airborne NP and MP groups

Multiple differential nasal bacteria and related microbial pathways were determined between AQ and AR groups (Supplementary Materials Fig. S12a and b). Among them, Rikenellaceae_RC9_gut_group and "vitamin B6 metabolism" could largely differentiate the AQ group from the AR group, while *Ileibacterium*

and "ABC transporters" could greatly distinguish the AR group from the AQ group (Supplementary Materials Fig. S12a and b). In contrast, only two differential lung bacteria, i.e., *Hungatella* and Lachnospiraceae_A2, were more enriched in the AQ and AR groups, respectively (Supplementary Materials Fig. S12c), and no lung microbial pathway differed between the two groups.

Among the 776 lung metabolites that differed between AQ and AR groups, 422 were more elevated in the AQ group, while 354 were at higher levels in the AR group (Supplementary Materials Fig. S12d). The two groups of lung metabolites were mainly involved in the upregulated pathways such as "arachidonic acid metabolism", "steroid hormone biosynthesis", and "ABC transporters" in the AQ group (Supplementary Materials Fig. S12e), and the upregulated pathways such as "purine metabolism" and "ABC transporters" in the AR group (Supplementary Materials Fig. S12f). Similarly, the serum metabolites differed between the AQ and AR groups; 66 were at higher levels in the AQ group, while 135 were more enriched in the AR group (Supplementary Materials Fig. S12g). These differential serum metabolites were mainly related to the more intensified serum pathways, such as "ABC transporters" and "purine metabolism" in the AQ group (Supplementary Materials Fig. S12h), and the more intensified serum pathways, such as "D-amino acid metabolism", "pentose phosphate pathway", and "central carbon metabolism in cancer" in the AR group (Supplementary Materials Fig. S12i). Multiple DEGs and differential GO terms were determined between AQ and AR groups (Supplementary Materials Fig. S12j and k), and they mainly contributed to the more enriched liver pathways "hematopoietic cell lineage" and "parathyroid hormone synthesis, secretion and action" in the AQ and AR groups, respectively (Supplementary Materials Fig. S12l and m).

4. Discussion

Eco-friendly materials have been used to decrease environmental pollution [20]. However, some of them can be toxic to human beings. Although foodborne and airborne MNPs can cause abnormal health conditions in multiple organisms [4,21], their toxic effects are still largely underestimated [22,23]. There is a lack of research about the amount and concentrations of PLA MNPs in the human living environment, which needs further exploration. An individual was estimated to ingest up to 5 g MNPs per week [5], and the MNP doses for the animal experiments in this study were below the amount. However, this amount could be largely underestimated due to inefficient MNP collection and quantification techniques [24,25]. This study found foodborne and airborne biodegradable PLA NPs and MPs to disrupt different microbiota-involved axes and induce hepatotoxicity.

In this study, foodborne and airborne PLA NPs and MPs were found to increase the serum AST and ALT and affect the serum SOD and T-AOC, suggesting the PLA MNP exposure could affect the liver function and serum antioxidant activity. Higher levels of AST and ALT and lower levels of SOD and T-AOC were determined in the serum of mice orally exposed to PS MPs [26]. Liver pathological changes (e.g., cell vacuolization and hepatocyte swelling) were found in the FQ, FR, AQ, and AR groups, suggesting that both foodborne and airborne PLA MNPs could impair the liver. Oral exposure to PS MPs could induce liver pathological changes such as hepatocyte edema, enlarged nuclei, and portal inflammation in mice [27]. Lung pathological changes, i.e., hemorrhage, inflammatory cell infiltration, and exudates, were determined in the AQ and AR groups, suggesting airborne PLA MNPs could impair the lung. PS MP nasal exposure was capable of causing inflammatory cell infiltration in the mouse liver [9].

FQ and FR groups differed from the FNC group in terms of the gut microbiota composition, suggesting that foodborne PLA NPs and MPs could alter the gut microbiota composition. PS MNP oral exposure was found to cause marked gut microbial dysbiosis [28]. The alpha diversity of gut microbiota was not significantly altered in the FQ and FR groups, suggesting PLA MNP oral exposure did not alter the gut microbial alpha diversity. This is different from previous studies, which determined that PE and PS MNP oral exposures can alter the alpha diversity of gut microbiota in mice [8,29]. Among the gut bacteria elevated in the FQ and FR groups, Lachnospiraceae_NK4A136_group, Lachnospiraceae_A2, and *Helicobacter* were greatly enriched in the FQ group, while Lachnospiraceae_NK4A136_group, *Roseburia*, and *Helicobacter* were largely enriched in the FR group. Gut Lachnospiraceae_NK4A136_group was more abundant in the mice orally exposed to PS MNPs compared to the control group [30]. Reduced Lachnospiraceae_A2 was found in the mice orally exposed to polychlorinated biphenyls [31]. *Helicobacter pylori* could cooperate with PE MPs to cause gastric injury in mice [32]. Less gut *Roseburia* was determined in the PS MNPs orally exposed mice compared to the control group [28]. Gut Lachnospiraceae_NK4A136_group was most upregulated in both FQ and FR groups, suggesting it is a potential biomarker of PLA MNP oral exposure.

Nasal microbiota composition differed between the AQ/AR and ANC groups, suggesting that airborne PLA NPs and MPs could cause nasal microbiota alterations. Airborne PS NPs and MPs were found to alter the nasal microbiota compositions in the exposed mice [10]. The nasal alpha diversity indices were all greater in the AQ and AR groups compared to the ANC group, suggesting PLA MNP nasal exposure could alter the nasal microbial alpha diversity, which is different from our previous study determining PS MNP nasal exposure not capable of altering nasal microbial alpha diversity in mice [10]. Among the multiple differential nasal bacteria between AQ and AR groups, unclassified_Muribaculaceae, *Acinetobacter*, and Lachnospiraceae_NK4A136_group were largely enriched in the AQ group, while unclassified_Muribaculaceae, *Lactobacillus*, and *Sporosarcina* were largely enriched in the AR group. Unclassified_Muribaculaceae was largely upregulated in the lung of mice nasally exposed to PS NPs [10]. *Acinetobacter* was at a greater level in the intestine of mice orally exposed to PS MPs compared to the control group [33]. The abundance of gut Lachnospiraceae_NK4A136_group could be augmented in the mice orally exposed to PS NPs and MPs [34]. Gut *Lactobacillus* was enriched in the foodborne PE MPs-exposed mice [35]. Increased gut *Sporosarcina* was determined in the PS MPs-exposed marine medaka [36]. Nasal unclassified_Muribaculaceae was most upregulated in both AQ and AR groups, suggesting it is a potential biomarker for PLA MNP nasal exposure.

The AQ and AR groups altered the lung microbiota composition compared to the ANC group, suggesting that airborne PLA NPs and MPs could induce lung microbiota alterations. Nasal exposures to PS NPs and MPs were found to change the lung microbiota compositions in mice [10]. As for the lung bacterial alpha diversity, reduced observed species in the AQ and AR groups, decreased Shannon index in the AR group, and elevated Pielou index in the AQ group was determined, suggesting that airborne PLA MNPs could alter the lung microbial diversity. Shannon index and observed species of lung microbiota were found at lower levels in the mice exposed to airborne PS MPs compared to the control group [10]. Multiple bacteria were enriched in the lungs of AQ and AR groups, among which *Klebsiella*, *Clostridium_sensu_stricto*_1, and *Escherichia-Shigella* were most associated with both the two groups. *Klebsiella pneumoniae* was determined to have the ability to degrade submicroplastics [37]. *Clostridium_sensu_stricto*_1 was reduced in the gut of PS NPs-exposed largemouth bass [38]. In the human placenta, *Escherichia-Shigella* was negatively correlated

with the PVC concentration but positively correlated with the polytetrafluoroethylene concentration [39]. Lung *Klebsiella* was most enriched in both AQ and AR groups, suggesting it is a potential biomarker for PLA MNP nasal exposure.

Multiple structural gatekeepers were found in the gut microbiota networks of FQ and FR groups, some of which (e.g., Lachnospiraceae and Oscillospiraceae) were found in both of the two networks. Reduced Lachnospiraceae was found in the intestine of PE MPs-exposed crayfish [40]. The abundance of gut Oscillospiraceae was augmented in the intestine of mice exposed to foodborne PS MPs [41]. Likewise, some nasal phylotypes assigned to bacteria, such as *Alistipes* and *Sphingomonas*, were determined as structural gatekeepers in the AQ and AR groups, respectively. Gut *Alistipes* was positively correlated with gastrointestinal dysfunction in the individuals consuming food in disposable plastic containers [42]. Nasal *Sphingomonas* was increased in the airborne PS MPs-treated mice [10].

Multiple gut/serum metabolic and liver transcriptomic alterations were determined in the FQ and FR groups, suggesting both foodborne PLA NPs and MPs could cause metabolic disruption and transcriptomic dysregulation in mice. Two groups of gut metabolic pathways were enriched in the FQ and FR groups, among which "central carbon metabolism in cancer" was largely enriched in both groups. "Central carbon metabolism in cancer" was enriched in the intestines of rats orally exposed to PS NPs [43]. Likewise, multiple serum metabolic pathways were enriched in the FQ and FR groups, of which "linoleic acid metabolism" was greatly enriched in both the two groups. "Linoleic acid metabolism" was enriched in the zebrafish embryos exposed to PS NPs and MPs [44]. Multiple liver pathways with enriched DEGs were found in the FQ and FR groups, the "circadian rhythm" of which was greatly enriched in both groups. PS NP oral exposure was found to induce neurotoxicity in mice by affecting pathways related to circadian rhythm [45]. The above three pathways, i.e., gut pathway "central carbon metabolism in cancer", serum pathway "linoleic acid metabolism", and liver pathway "circadian rhythm", could be vital to the liver toxicity of foodborne PLA MNPs. We acknowledge they need to be further investigated.

Various lung/serum metabolites and liver transcripts were altered in the AQ and AR groups, suggesting both airborne PLA NPs and MPs could induce metabolic disruption and transcriptomic dysregulation in mice. "Arachidonic acid metabolism" was the lung pathway most enriched in both AQ and AR groups, while "protein digestion and absorption" and "central carbon metabolism in cancer" were the two serum pathways greatly enriched in both AQ and AR groups. Abnormal "arachidonic acid metabolism" was determined in the PS NPs-exposed earthworms [46]. "Protein digestion and absorption" was enriched in *Ietalurus punetaus* larvae exposed to PS NPs [47]. "Central carbon metabolism in cancer" was upregulated in PE MPs-exposed *Daphnia magna* [48]. Among the multiple liver pathways enriched in the AQ and AR groups, "alcoholism", "systemic lupus erythematosus", and "neutrophil extracellular trap formation" were largely enriched in both groups. "MAPK signaling pathway" was involved in chronic ethanol-induced alcoholism, which was associated with the reproductive toxicity caused by PS MP oral exposure [49]. MPs could be a particular matter in the air and induce autoimmune diseases such as lupus erythematosus [50]. PS NP exposure could induce neutrophil extracellular traps in mouse neutrophils [51]. Lung pathway "arachidonic acid metabolism", serum pathways "central carbon metabolism in cancer" and "protein digestion and absorption", and liver pathway "alcoholism" were largely enriched in both AQ and AR groups, suggesting they could be important to the hepatotoxicity of airborne PLA MNPs. We acknowledge they deserve further exploration.

Multiple correlations were determined between the altered components (i.e., microbes, metabolites, and transcripts) in the MNP groups, and some components played vital roles in the correlation networks: DEG *Gm1673* in the FQ group; DEGs *cyp2b9* and *klhdc7b*, and serum metabolite bacterioruberin diglucoside in the FR group; DEG *zfp804b* in the AQ group; and gut metabolite 11-cis-3,4-didehydroretinol in the AR group. *Gm1673* was found overexpressed in the nucleus accumbens of nitroglycerin-treated mice [52]. *Cyp2b9* could be increased in the liver of mice orally exposed to PVC MPs [53]. *Klhdc7b* was enriched in breast cancer tissue and cells [54]. *Zfp804b* encoded zinc finger proteins could be increased by maternal fluoxetine exposure [55]. Cyp27c1 was found to converse 11-cis retinal to 11-cis-3,4-didehydroretinal in the eye of zebrafish [56]. Some pathways were enriched in more than one organ and/or serum of the FQ, FR, AQ, or AR groups, and "circadian rhythm" was commonly enriched in the liver of the four groups. These pathways were likely to play vital roles in the liver toxicity induced by foodborne and airborne PLA NPs and MPs, and we acknowledge that they need to be further investigated in future work.

Multiple factors could differentiate foodborne PLA NP and MP exposures. The two differential gut bacteria between the FQ and FR groups, i.e., Lachnospiraceae_A2 and *Roseburia*, were greatly more enriched in the FQ and FR groups, respectively. They have been mentioned earlier in this Discussion section for their associations with MNPs [28,31]. Six gut pathways were at different levels between the FQ and FR groups, and all of them were more enriched in the FQ group, among which "glycolysis/gluconeogenesis" was most enriched. Maternal PS MP exposure could disturb "glycolysis/gluconeogenesis" in the placenta of pregnant mice [57]. Among the multiple differential serum and liver pathways between FQ and FR groups, "glycerophospholipid metabolism" in serum and "acute myeloid leukemia" in the liver were greatly more enriched in the FQ group, while serum pathway "choline metabolism in cancer" and liver pathway "retinol metabolism" were largely more enriched in the FR group. Disrupted "glycerophospholipid metabolism" was found in the gut of zebrafish exposed to a higher dose of polypropylene (PP) MPs (100 μg L^{-1}) [58]. Increased occurrence of acute myeloid leukemia has been found in workers exposed to high levels of styrene [59]. "Choline metabolism in cancer" could be enriched in the *Daphnia magna* exposed to PE MPs [48]. "Retinol metabolism" in the mouse liver was disrupted by the PS MP oral exposure [12].

Likewise, multiple factors could differentiate airborne PLA NP and MP exposures. Among the differential airway bacteria between the AQ and AR groups, nasal Rikenellaceae_RC9_gut_group and lung *Hungatella* were greatly increased in the AQ group, while nasal *Ileibacterium* and lung Lachnospiraceae_A2 were largely elevated in the AP group. Rikenellaceae_RC9_gut_group was overrepresented in the intestines of zebrafish exposed to commercial PS MPs [60]. *Hungatella* was at a higher level in the gut of PLA MPs-exposed silkworm than the control group [61]. Gut *Ileibacterium* was enriched in the foodborne PS MPs-exposed mice [41]. A shifted light-dark cycle could cause circadian disruption-induced metabolic syndrome via modulating the gut microbiota in mice, e.g., downregulation of Lachnospiraceae_A2 [62]. A variety of differential lung, serum, and liver pathways were found between the AQ and AR groups. Some of these differential pathways were more enriched in the AQ group, e.g., lung and serum pathway "ABC transporters" and liver pathway "hematopoietic cell lineage", while some alternative differential pathways were more enriched in the AR group, e.g., lung pathway "purine metabolism", serum pathway "D-amino acid metabolism", and liver pathway "parathyroid hormone synthesis, secretion, and action". PS NP exposure could enhance arsenic toxicity to AGS cells by disturbing the activity of

ABC transporters [63], and it could induce genotoxicity in the hematopoietic cell lines [64]. Exposure to PS NPs could upregulate "purine metabolism" in the muscle of razor clams [65]. PE MP oral exposure could enrich "D-amino acid metabolism" in the chicken's intestine [66]. Copper oxide NP exposure enriched "parathyroid hormone synthesis, secretion, and action" in the human placenta [67].

5. Conclusion

In summary, foodborne and airborne PLA NPs and MPs could cause microbiota alteration, metabolic disruption, and transcriptomic dysregulation in mice. PLA MNP oral exposure could disrupt the "gut microbiota-gut-liver" axis and induce hepatotoxicity, while PLA MNP nasal exposure could influence the "airway microbiota-lung-liver" axis and cause hepatotoxicity. The relevant findings could benefit the clinical diagnosis of hepatotoxicity induced by foodborne and airborne PLA MNPs and the proper use of biodegradable materials in the environment.

CRediT authorship contribution statement

Hua Zha: Conceptualization, Formal Analysis, Funding Acquisition, Investigation, Methodology, Writing - Original Draft, Writing - Review & Editing. **Shengyi Han:** Data Curation, Investigation. **Ruiqi Tang:** Investigation, Methodology. **Dan Cao:** Investigation. **Kevin Chang:** Writing - Review & Editing. **Lanjuan Li:** Funding Acquisition, Project Administration, Resources, Supervision, Writing - Original Draft, Writing - Review & Editing.

Declaration of competing interest

The authors declare that they have no known competing financial interests or personal relationships that could have appeared to influence the work reported in this paper.

Acknowledgements

This work was supported by the National Natural Science Foundation of China (82003441).

Appendix A. Supplementary data

Supplementary data to this article can be found online at https://doi.org/10.1016/j.ese.2024.100428.

References

[1] T. Bagheri, M. Gholizadeh, S. Abarghouei, M. Zakeri, A. Hedayati, M. Rabaniha, A. Aghaeimoghadam, M. Hafezieh, Microplastics distribution, abundance and composition in sediment, fishes and benthic organisms of the Gorgan Bay, Caspian sea, Chemosphere 257 (2020) 127201.
[2] S. Marano, E. Laudadio, C. Minnelli, P. Stipa, Tailoring the barrier properties of PLA: a state-of-the-art review for food packaging applications, Polymers 14 (8) (2022) 1626.
[3] G. Banaei, A. García-Rodríguez, A. Tavakolpournegari, J. Martín-Pérez, A. Villacorta, R. Marcos, A. Hernández, The release of polylactic acid nanoplastics (PLA-NPLs) from commercial teabags. Obtention, characterization, and hazard effects of true-to-life PLA-NPLs, J. Hazard. Mater. (2023) 131899.
[4] F. Yu, Y. Pei, X. Zhang, J. Ma, Weathering and degradation of polylactic acid masks in a simulated environment in the context of the COVID-19 pandemic and their effects on the growth of winter grazing ryegrass, J. Hazard. Mater. 448 (2023) 130889.
[5] K. Senathirajah, S. Attwood, G. Bhagwat, M. Carbery, S. Wilson, T. Palanisami, Estimation of the mass of microplastics ingested—A pivotal first step towards human health risk assessment, J. Hazard. Mater. 404 (2021) 124004.
[6] R. Qiao, Y. Deng, S. Zhang, M.B. Wolosker, Q. Zhu, H. Ren, Y. Zhang, Accumulation of different shapes of microplastics initiates intestinal injury and gut microbiota dysbiosis in the gut of zebrafish, Chemosphere 236 (2019) 124334.
[7] Y. Zhou, C. Wu, Y. Li, H. Jiang, A. Miao, Y. Liao, K. Pan, Effects of nanoplastics on clam *Ruditapes philippinarum* at environmentally realistic concentrations: toxicokinetics, toxicity, and gut microbiota, J. Hazard. Mater. 456 (2023) 131647.
[8] B. Li, Y. Ding, X. Cheng, D. Sheng, Z. Xu, Q. Rong, Y. Wu, H. Zhao, X. Ji, Y. Zhang, Polyethylene microplastics affect the distribution of gut microbiota and inflammation development in mice, Chemosphere 244 (2020) 125492.
[9] K. Lu, K.P. Lai, T. Stoeger, S. Ji, Z. Lin, X. Lin, T.F. Chan, J.K.-H. Fang, M. Lo, L. Gao, Detrimental effects of microplastic exposure on normal and asthmatic pulmonary physiology, J. Hazard. Mater. 416 (2021) 126069.
[10] H. Zha, J. Xia, S. Li, J. Lv, A. Zhuge, R. Tang, S. Wang, K. Wang, K. Chang, L. Li, Airborne polystyrene microplastics and nanoplastics induce nasal and lung microbial dysbiosis in mice, Chemosphere 310 (2023) 136764.
[11] M. Xu, G. Halimu, Q. Zhang, Y. Song, X. Fu, Y. Li, Y. Li, H. Zhang, Internalization and toxicity: a preliminary study of effects of nanoplastic particles on human lung epithelial cell, Sci. Total Environ. 694 (2019) 133794.
[12] C. Shi, X. Han, W. Guo, Q. Wu, X. Yang, Y. Wang, G. Tang, S. Wang, Z. Wang, Y. Liu, Disturbed Gut-Liver axis indicating oral exposure to polystyrene microplastic potentially increases the risk of insulin resistance, Environ. Int. 164 (2022) 107273.
[13] R. Dong, C. Zhou, S. Wang, Y. Yan, Q. Jiang, Probiotics ameliorate polyethylene microplastics-induced liver injury by inhibition of oxidative stress in Nile tilapia (*Oreochromis niloticus*), Fish Shellfish Immunol. 130 (2022) 261—272.
[14] S. Wen, Y. Zhao, S. Liu, Y. Chen, H. Yuan, H. Xu, Polystyrene microplastics exacerbated liver injury from cyclophosphamide in mice: insight into gut microbiota, Sci. Total Environ. 840 (2022) 156668.
[15] Z. Duan, H. Cheng, X. Duan, H. Zhang, Y. Wang, Z. Gong, H. Zhang, H. Sun, L. Wang, Diet preference of zebrafish (*Danio rerio*) for bio-based polylactic acid microplastics and induced intestinal damage and microbiota dysbiosis, J. Hazard. Mater. 429 (2022) 128332.
[16] T.Q. Chagas, A.P. da Costa Araújo, G. Malafaia, Biomicroplastics versus conventional microplastics: an insight on the toxicity of these polymers in dragonfly larvae, Sci. Total Environ. 761 (2021) 143231.
[17] H. Zha, Q. Li, K. Chang, J. Xia, S. Li, R. Tang, L. Li, Characterising the intestinal bacterial and fungal microbiome associated with different cytokine profiles in two bifidobacterium strains pre-treated rats with D-galactosamine-induced liver injury, Front. Immunol. 13 (2022) 791152.
[18] B.J. Callahan, P.J. McMurdie, M.J. Rosen, A.W. Han, A.J.A. Johnson, S.P. Holmes, DADA2: high-resolution sample inference from Illumina amplicon data, Nat. Methods 13 (7) (2016) 581—583.
[19] M.S. Dueholm, K.S. Andersen, S.J. McIlroy, J.M. Kristensen, E. Yashiro, S.M. Karst, M. Albertsen, P.H. Nielsen, Generation of comprehensive ecosystem-specific reference databases with species-level resolution by high-throughput full-length 16S rRNA gene sequencing and automated taxonomy assignment (AutoTax), mBio 11 (5) (2020) e0155720.
[20] M.R. Pahlevi, D. Suhartanto, The integrated model of green loyalty: evidence from eco-friendly plastic products, J. Clean. Prod. 257 (2020) 120844.
[21] D. Huang, J. Tao, M. Cheng, R. Deng, S. Chen, L. Yin, R. Li, Microplastics and nanoplastics in the environment: macroscopic transport and effects on creatures, J. Hazard. Mater. 407 (2021) 124399.
[22] B. Liang, Y. Zhong, Y. Huang, X. Lin, J. Liu, L. Lin, M. Hu, J. Jiang, M. Dai, B. Wang, Underestimated health risks: polystyrene micro-and nanoplastics jointly induce intestinal barrier dysfunction by ROS-mediated epithelial cell apoptosis, Part. Fibre Toxicol. 18 (1) (2021) 20.
[23] L. Lv, H. Jiang, R. Yan, L. Li, Interactions between gut microbiota and hosts and their role in infectious diseases, Infect. Microbes Dis. 1 (1) (2019) 3—9.
[24] M.J. Huber, N.P. Ivleva, A.M. Booth, I. Beer, I. Bianchi, R. Drexel, O. Geiss, D. Mehn, F. Meier, A. Molska, Physicochemical characterization and quantification of nanoplastics: applicability, limitations and complementarity of batch and fractionation methods, Anal. Bioanal. Chem. 415 (2023) 3007—3031.
[25] Y. Xie, Y. Li, Y. Feng, W. Cheng, Y. Wang, Inhalable microplastics prevails in air: exploring the size detection limit, Environ. Int. 162 (2022) 107151.
[26] H. Zou, H. Qu, Y. Bian, J. Sun, T. Wang, Y. Ma, Y. Yuan, J. Gu, J. Bian, Z. Liu, Polystyrene microplastics induce oxidative stress in mouse hepatocytes in relation to their size, Int. J. Mol. Sci. 24 (8) (2023) 7382.
[27] R. Shen, K. Yang, X. Cheng, C. Guo, X. Xing, H. Sun, D. Liu, X. Liu, D. Wang, Accumulation of polystyrene microplastics induces liver fibrosis by activating cGAS/STING pathway, Environ. Pollut. 300 (2022) 118986.
[28] J. Qiao, R. Chen, M. Wang, R. Bai, X. Cui, Y. Liu, C. Wu, C. Chen, Perturbation of gut microbiota plays an important role in micro/nanoplastics-induced gut barrier dysfunction, Nanoscale 13 (19) (2021) 8806—8816.
[29] Y. Jin, L. Lu, W. Tu, T. Luo, Z. Fu, Impacts of polystyrene microplastic on the gut barrier, microbiota and metabolism of mice, Sci. Total Environ. 649 (2019) 308—317.
[30] J. Jing, L. Zhang, L. Han, J. Wang, W. Zhang, Z. Liu, A. Gao, Polystyrene micro-/nanoplastics induced hematopoietic damages via the crosstalk of gut microbiota, metabolites, and cytokines, Environ. Int. 161 (2022) 107131.
[31] J.J. Lim, X. Li, H.-J. Lehmler, D. Wang, H. Gu, J.Y. Cui, Gut microbiome critically impacts PCB-induced changes in metabolic fingerprints and the hepatic transcriptome in mice, Toxicol. Sci. 177 (1) (2020) 168—187.
[32] X. Tong, B. Li, J. Li, L. Li, R. Zhang, Y. Du, Y. Zhang, Polyethylene microplastics cooperate with Helicobacter pylori to promote gastric injury and inflammation in mice, Chemosphere 288 (2022) 132579.
[33] L. Lu, Z. Wan, T. Luo, Z. Fu, Y. Jin, Polystyrene microplastics induce gut microbiota dysbiosis and hepatic lipid metabolism disorder in mice, Sci. Total

Environ. 631 (2018) 449–458.
[34] X. Chen, L. Xu, Q. Chen, S. Su, J. Zhuang, D. Qiao, Polystyrene micro-and nanoparticles exposure induced anxiety-like behaviors, gut microbiota dysbiosis and metabolism disorder in adult mice, Ecotoxicol. Environ. Saf. 259 (2023) 115000.
[35] Y. Deng, Z. Yan, R. Shen, M. Wang, Y. Huang, H. Ren, Y. Zhang, B. Lemos, Microplastics release phthalate esters and cause aggravated adverse effects in the mouse gut, Environ. Int. 143 (2020) 105916.
[36] X. Zhang, K. Wen, D. Ding, J. Liu, Z. Lei, X. Chen, G. Ye, J. Zhang, H. Shen, C. Yan, Size-dependent adverse effects of microplastics on intestinal microbiota and metabolic homeostasis in the marine medaka (*Oryzias melastigma*), Environ. Int. 151 (2021) 106452.
[37] H. Saygin, A. Baysal, Insights into the degradation behavior of submicroplastics by Klebsiella pneumoniae, J. Polym. Environ. 29 (2021) 958–966.
[38] M. Chen, Y. Yue, X. Bao, X. Feng, Z. Ou, Y. Qiu, K. Yang, Y. Yang, Y. Yu, H. Yu, Effects of polystyrene nanoplastics on oxidative stress, histopathology and intestinal microbiota in largemouth bass (*Micropterus salmoides*), Aquacult. Res. 27 (2022) 101423.
[39] S. Liu, X. Liu, J. Guo, R. Yang, H. Wang, Y. Sun, B. Chen, R. Dong, The association between microplastics and microbiota in placentas and meconium: the first evidence in humans, Environ. Sci. Technol. (2023) in press.
[40] X. Zhang, Z. Jin, M. Shen, Z. Chang, G. Yu, L. Wang, X. Xia, Accumulation of polyethylene microplastics induces oxidative stress, microbiome dysbiosis and immunoregulation in crayfish, Fish Shellfish Immunol. 125 (2022) 276–284.
[41] W. Chen, R. Zhu, X. Ye, Y. Sun, Q. Tang, Y. Liu, F. Yan, T. Yu, X. Zheng, P. Tu, Food-derived cyanidin-3-O-glucoside reverses microplastic toxicity via promoting discharge and modulating the gut microbiota in mice, Food Funct. 13 (3) (2022) 1447–1458.
[42] H. Zha, J. Lv, Y. Lou, W. Wo, J. Xia, S. Li, A. Zhuge, R. Tang, N. Si, Z. Hu, Alterations of gut and oral microbiota in the individuals consuming take-away food in disposable plastic containers, J. Hazard. Mater. 441 (2023) 129903.
[43] W. Jiang, C. Hu, Y. Chen, Y. Li, X. Sun, H. Wu, R. Yang, Y. Tang, F. Niu, W. Wei, Dysregulation of the microbiota-brain axis during long-term exposure to polystyrene nanoplastics in rats and the protective role of dihydrocaffeic acid, Sci. Total Environ. 874 (2023) 162101.
[44] Z. Duan, X. Duan, S. Zhao, X. Wang, J. Wang, Y. Liu, Y. Peng, Z. Gong, L. Wang, Barrier function of zebrafish embryonic chorions against microplastics and nanoplastics and its impact on embryo development, J. Hazard. Mater. 395 (2020) 122621.
[45] H. Kang, W. Zhang, J. Jing, D. Huang, L. Zhang, J. Wang, L. Han, Z. Liu, Z. Wang, A. Gao, The gut-brain axis involved in polystyrene nanoplastics-induced neurotoxicity via reprogramming the circadian rhythm-related pathways, J. Hazard. Mater. 458 (2023) 131949.
[46] R. Tang, D. Zhu, Y. Luo, D. He, H. Zhang, A. El-Naggar, K.N. Palansooriya, K. Chen, Y. Yan, X. Lu, Nanoplastics induce molecular toxicity in earthworm: integrated multi-omics, morphological, and intestinal microorganism analyses, J. Hazard. Mater. 442 (2023) 130034.
[47] Q. Jiang, X. Chen, H. Jiang, M. Wang, T. Zhang, W. Zhang, Effects of acute exposure to polystyrene nanoplastics on the channel catfish larvae: insights from energy metabolism and transcriptomic analysis, Front. Physiol. 13 (2022) 923278.
[48] P. Wang, Q. Li, J. Hui, Q. Xiang, H. Yan, L. Chen, Metabolomics reveals the mechanism of polyethylene microplastic toxicity to *Daphnia magna*, Chemosphere 307 (2022) 135887.
[49] X. Xie, T. Deng, J. Duan, J. Xie, J. Yuan, M. Chen, Exposure to polystyrene microplastics causes reproductive toxicity through oxidative stress and activation of the p38 MAPK signaling pathway, Ecotoxicol. Environ. Saf. 190 (2020) 110133.
[50] H.K. Ageel, S. Harrad, M.A.-E. Abdallah, Occurrence, human exposure, and risk of microplastics in the indoor environment, Environ. Sci.: Process. Impacts 24 (1) (2022) 17–31.
[51] X. Zhu, L. Peng, E. Song, Y. Song, Polystyrene nanoplastics induce neutrophil extracellular traps in mice neutrophils, Chem. Res. Toxicol. 35 (3) (2022) 378–382.
[52] H. Jeong, L.S. Moye, B.R. Southey, A.G. Hernandez, I. Dripps, E.V. Romanova, S.S. Rubakhin, J.V. Sweedler, A.A. Pradhan, S.L. Rodriguez-Zas, Gene network dysregulation in the trigeminal ganglia and nucleus accumbens of a model of chronic migraine-associated hyperalgesia, Front. Syst. Neurosci. 12 (2018) 63.
[53] X. Chen, J. Zhuang, Q. Chen, L. Xu, X. Yue, D. Qiao, Chronic exposure to polyvinyl chloride microplastics induces liver injury and gut microbiota dysbiosis based on the integration of liver transcriptome profiles and full-length 16S rRNA sequencing data, Sci. Total Environ. 839 (2022) 155984.
[54] T.W. Kim, Y.J. Kim, H.J. Lee, S.Y. Min, H.-S. Kang, S.J. Kim, Hs. 137007 is a novel epigenetic marker hypermethylated and up-regulated in breast cancer, Int. J. Oncol. 36 (5) (2010) 1105–1111.
[55] H.E. Vuong, E.J. Coley, M. Kazantsev, M.E. Cooke, T.K. Rendon, J. Paramo, E.Y. Hsiao, Interactions between maternal fluoxetine exposure, the maternal gut microbiome and fetal neurodevelopment in mice, Behav. Brain Res. 410 (2021) 113353.
[56] J.M. Enright, M.B. Toomey, S.-y. Sato, S.E. Temple, J.R. Allen, R. Fujiwara, V.M. Kramlinger, L.D. Nagy, K.M. Johnson, Y. Xiao, Cyp27c1 red-shifts the spectral sensitivity of photoreceptors by converting vitamin A1 into A2, Curr. Biol. 25 (23) (2015) 3048–3057.
[57] Z. Aghaei, G.V. Mercer, C.M. Schneider, J.G. Sled, C.K. Macgowan, A.A. Baschat, J.C. Kingdom, P.A. Helm, A.J. Simpson, M.J. Simpson, Maternal exposure to polystyrene microplastics alters placental metabolism in mice, Metabolomics 19 (1) (2022) 1.
[58] Y. Zhao, R. Qiao, S. Zhang, G. Wang, Metabolomic profiling reveals the intestinal toxicity of different length of microplastic fibers on zebrafish (*Danio rerio*), J. Hazard. Mater. 403 (2021) 123663.
[59] M.S. Christensen, J.M. Vestergaard, F. d'Amore, J.S. Gørløv, G. Toft, C.H. Ramlau-Hansen, Z.A. Stokholm, I.B. Iversen, M.S. Nissen, H.A. Kolstad, Styrene exposure and risk of lymphohematopoietic malignancies in 73,036 reinforced plastics workers, Epidemiology 29 (3) (2018) 342–351.
[60] X. Guo, M. Lv, J. Li, J. Ding, Y. Wang, L. Fu, X. Sun, X. Han, L. Chen, The distinct toxicity effects between commercial and realistic polystyrene microplastics on microbiome and histopathology of gut in zebrafish, J. Hazard. Mater. 434 (2022) 128874.
[61] X. Wu, X. Zhang, X. Chen, A. Ye, J. Cao, X. Hu, W. Zhou, The effects of polylactic acid bioplastic exposure on midgut microbiota and metabolite profiles in silkworm (*Bombyx mori*): an integrated multi-omics analysis, Environ. Pollut. 334 (2023) 122210.
[62] W. Cheng, K. Lam, X. Li, A.P. Kong, P.C. Cheung, Circadian disruption-induced metabolic syndrome in mice is ameliorated by oat β-glucan mediated by gut microbiota, Carbohydr. Polym. 267 (2021) 118216.
[63] P. Lin, Y. Guo, L. He, X. Liao, X. Chen, L. He, Z. Lu, Z.-J. Qian, C. Zhou, P. Hong, Nanoplastics aggravate the toxicity of arsenic to AGS cells by disrupting ABC transporter and cytoskeleton, Ecotoxicol. Environ. Saf. 227 (2021) 112885.
[64] L. Rubio, I. Barguilla, J. Domenech, R. Marcos, A. Hernández, Biological effects, including oxidative stress and genotoxic damage, of polystyrene nanoparticles in different human hematopoietic cell lines, J. Hazard. Mater. 398 (2020) 122900.
[65] Q. Jiang, W. Zhang, Gradual effects of gradient concentrations of polystyrene nanoplastics on metabolic processes of the razor clams, Environ. Pollut. 287 (2021) 117631.
[66] A. Li, Y. Wang, M.F.-E.-A. Kulyar, M. Iqbal, R. Lai, H. Zhu, K. Li, Environmental microplastics exposure decreases antioxidant ability, perturbs gut microbial homeostasis and metabolism in chicken, Sci. Total Environ. 856 (2023) 159089.
[67] S. Chortarea, G. Gupta, L. Saarimäki, W. Netkueakul, P. Manser, L. Aengenheister, A. Wichser, V. Fortino, P. Wick, D. Greco, Transcriptomic profiling reveals differential cellular response to copper oxide nanoparticles and polystyrene nanoplastics in perfused human placenta, Environ. Int. 177 (2023) 108015.